

Chapter 5

Dynamic Stability

These notes provide a brief background for the response of linear systems, with application to the equations of motion for a flight vehicle. The description is meant to provide the basic background in linear algebra for understanding modern tools for analyzing the response of linear systems, and provide examples of their application to flight vehicle dynamics. Examples for both longitudinal and lateral/directional motions are provided, and simple, lower-order approximations to the various modes are used to elucidate the roles of relevant aerodynamic properties of the vehicle.

5.1 Mathematical Background

5.1.1 An Introductory Example

The most interesting aircraft motions consist of oscillatory modes, the basic features of which can be understood by considering the simple system, sketched in Fig. 5.1, consisting of a spring, mass, and damper.

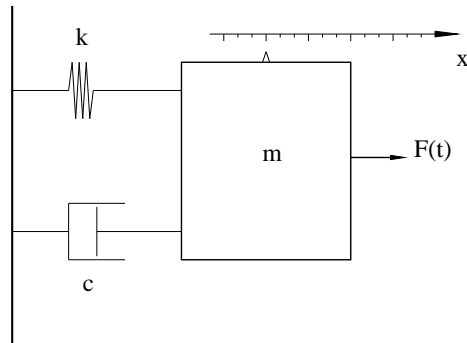


Figure 5.1: Schematic of spring-mass-damper system.

The dynamics of this system are described by the second-order ordinary differential equation

$$m \frac{d^2x}{dt^2} + c \frac{dx}{dt} + kx = F(t) \quad (5.1)$$

where m is the mass of the system, c is the damping parameter, and k is the spring constant of the restoring force. We generally are interested in both the *free response* of the system to an initial perturbation (with $F(t) = 0$), and the *forced response* to time-varying $F(t)$. The free response is relevant to the question of stability – i.e., the response to an infinitesimal perturbation from an equilibrium state of the system, while the forced response is relevant to control response.

The free response is the solution to the homogeneous equation, which can be written

$$\frac{d^2x}{dt^2} + \left(\frac{c}{m}\right) \frac{dx}{dt} + \left(\frac{k}{m}\right)x = 0 \quad (5.2)$$

Solutions of this equation are generally of the form

$$x = Ae^{\lambda t} \quad (5.3)$$

where A is a constant determined by the initial perturbation. Substitution of Eq. (5.3) into the differential equation yields the *characteristic equation*

$$\lambda^2 + \left(\frac{c}{m}\right)\lambda + \left(\frac{k}{m}\right) = 0 \quad (5.4)$$

which has roots

$$\lambda = -\frac{c}{2m} \pm \sqrt{\left(\frac{c}{2m}\right)^2 - \left(\frac{k}{m}\right)} \quad (5.5)$$

The nature of the response depends on whether the second term in the above expression is real or imaginary, and therefore depends on the relative magnitudes of the damping parameter c and the spring constant k . We can re-write the characteristic equation in terms of a variable defined by the ratio of the two terms in the square root

$$\frac{\left(\frac{c}{2m}\right)^2}{\left(\frac{k}{m}\right)} = \frac{c^2}{4mk} \equiv \zeta^2 \quad (5.6)$$

and a variable explicitly depending on the spring constant k , which we will choose (for reasons that will become obvious later) to be

$$\frac{k}{m} \equiv \omega_n^2 \quad (5.7)$$

In terms of these new variables, the original Eq. (5.2) can be written as

$$\frac{d^2x}{dt^2} + 2\zeta\omega_n \frac{dx}{dt} + \omega_n^2 x = 0 \quad (5.8)$$

The corresponding characteristic equation takes the form

$$\lambda^2 + 2\zeta\omega_n\lambda + \omega_n^2 = 0 \quad (5.9)$$

and its roots can now be written in the suggestive forms

$$\lambda = \begin{cases} -\zeta\omega_n \pm \omega_n\sqrt{\zeta^2 - 1} & \text{for } \zeta > 1 \\ -\zeta\omega_n & \text{for } \zeta = 1 \\ -\zeta\omega_n \pm i\omega_n\sqrt{1 - \zeta^2} & \text{for } \zeta < 1 \end{cases} \quad (5.10)$$

Overdamped System

For cases in which $\zeta > 1$, the characteristic equation has two (distinct) real roots, and the solution takes the form

$$x = a_1 e^{\lambda_1 t} + a_2 e^{\lambda_2 t} \quad (5.11)$$

where

$$\begin{aligned} \lambda_1 &= -\omega_n \left(\zeta + \sqrt{\zeta^2 - 1} \right) \\ \lambda_2 &= -\omega_n \left(\zeta - \sqrt{\zeta^2 - 1} \right) \end{aligned} \quad (5.12)$$

The constants a_1 and a_2 are determined from the initial conditions

$$\begin{aligned} x(0) &= a_1 + a_2 \\ \dot{x}(0) &= a_1 \lambda_1 + a_2 \lambda_2 \end{aligned} \quad (5.13)$$

or, in matrix form,

$$\begin{pmatrix} 1 & 1 \\ \lambda_1 & \lambda_2 \end{pmatrix} \begin{pmatrix} a_1 \\ a_2 \end{pmatrix} = \begin{pmatrix} x(0) \\ \dot{x}(0) \end{pmatrix} \quad (5.14)$$

Since the determinant of the coefficient matrix in these equations is equal to $\lambda_2 - \lambda_1$, the coefficient matrix is non-singular so long as the characteristic values λ_1 and λ_2 are distinct – which is guaranteed by Eqs. (5.12) when $\zeta > 1$. Thus, for the *overdamped* system ($\zeta > 1$), the solution is completely determined by the initial values of x and \dot{x} , and consists of a linear combination of two decaying exponentials.

The reciprocal of the *undamped natural frequency* ω_n forms a natural time scale for this problem, so if we introduce the dimensionless time

$$\hat{t} = \omega_n t \quad (5.15)$$

then Eq. (5.8) can be written

$$\frac{d^2 x}{d\hat{t}^2} + 2\zeta \frac{dx}{d\hat{t}} + x = 0 \quad (5.16)$$

which is seen to depend only on the damping ratio ζ . Figure 5.2 shows the response of overdamped systems for various values of the damping ratio as functions of the dimensionless time \hat{t} .

Critically Damped System

When the damping ratio $\zeta = 1$, the system is said to be *critically damped*, and there is only a single characteristic value

$$\lambda_1 = \lambda_2 = -\omega_n \quad (5.17)$$

Thus, only one of the two initial conditions can, in general, be satisfied by a solution of the form $e^{\lambda t}$. However, in this special case it is easily verified that $te^{\lambda t} = te^{-\omega_n t}$ is also a solution of Eq. (5.8), so the general form of the solution for the critically damped case can be written as

$$x = (a_1 + a_2 t) e^{-\omega_n t} \quad (5.18)$$

The constants a_1 and a_2 are again determined from the initial conditions

$$\begin{aligned} x(0) &= a_1 \\ \dot{x}(0) &= a_1 \lambda_1 + a_2 \end{aligned} \quad (5.19)$$

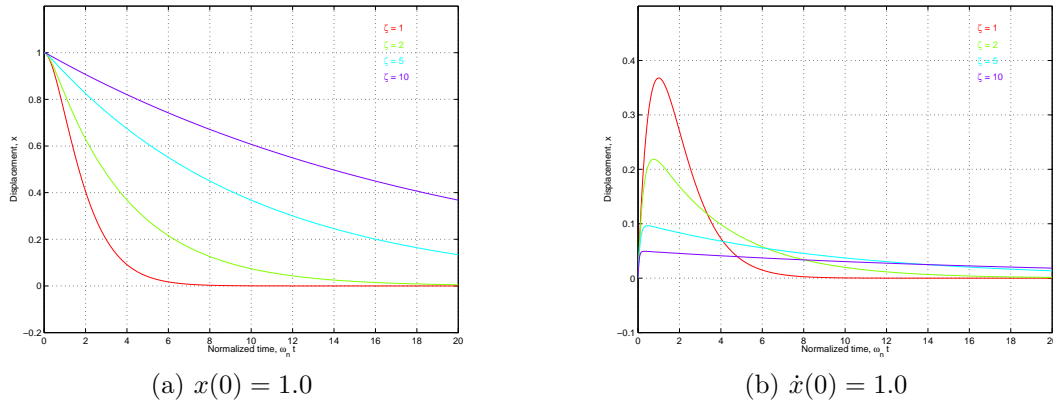


Figure 5.2: Overdamped response of spring-mass-damper system. (a) Displacement perturbation: $x(0) = 1.0$; $\dot{x}(0) = 0$. (b) Velocity perturbation: $\dot{x}(0) = 1.0$; $x(0) = 0$.

or, in matrix form,

$$\begin{pmatrix} 1 & 0 \\ \lambda_1 & 1 \end{pmatrix} \begin{pmatrix} a_1 \\ a_2 \end{pmatrix} = \begin{pmatrix} x(0) \\ \dot{x}(0) \end{pmatrix} \quad (5.20)$$

Since the determinant of the coefficient matrix in these equations is always equal to unity, the coefficient matrix is non-singular. Thus, for the *critically damped* system ($\zeta = 1$), the solution is again completely determined by the initial values of x and \dot{x} , and consists of a linear combination of a decaying exponential and a term proportional to $te^{-\omega_n t}$. For any positive value of ω_n the exponential decays more rapidly than any positive power of t , so the solution again decays, *nearly* exponentially.

Figures 5.2 and 5.3 include the limiting case of critically damped response for Eq. (5.16).

Underdamped System

When the damping ratio $\zeta < 1$, the system is said to be *underdamped*, and the roots of the characteristic equation consist of the complex conjugate pair

$$\begin{aligned} \lambda_1 &= \omega_n \left(-\zeta + i\sqrt{1-\zeta^2} \right) \\ \lambda_2 &= \omega_n \left(-\zeta - i\sqrt{1-\zeta^2} \right) \end{aligned} \quad (5.21)$$

Thus, the general form of the solution can be written

$$x = e^{-\zeta\omega_n t} \left[a_1 \cos \left(\omega_n \sqrt{1-\zeta^2} t \right) + a_2 \sin \left(\omega_n \sqrt{1-\zeta^2} t \right) \right] \quad (5.22)$$

The constants a_1 and a_2 are again determined from the initial conditions

$$\begin{aligned} x(0) &= a_1 \\ \dot{x}(0) &= -\zeta\omega_n a_1 + \omega_n \sqrt{1-\zeta^2} a_2 \end{aligned} \quad (5.23)$$

or, in matrix form,

$$\begin{pmatrix} 1 & 0 \\ -\zeta\omega_n & \omega_n \sqrt{1-\zeta^2} \end{pmatrix} \begin{pmatrix} a_1 \\ a_2 \end{pmatrix} = \begin{pmatrix} x(0) \\ \dot{x}(0) \end{pmatrix} \quad (5.24)$$

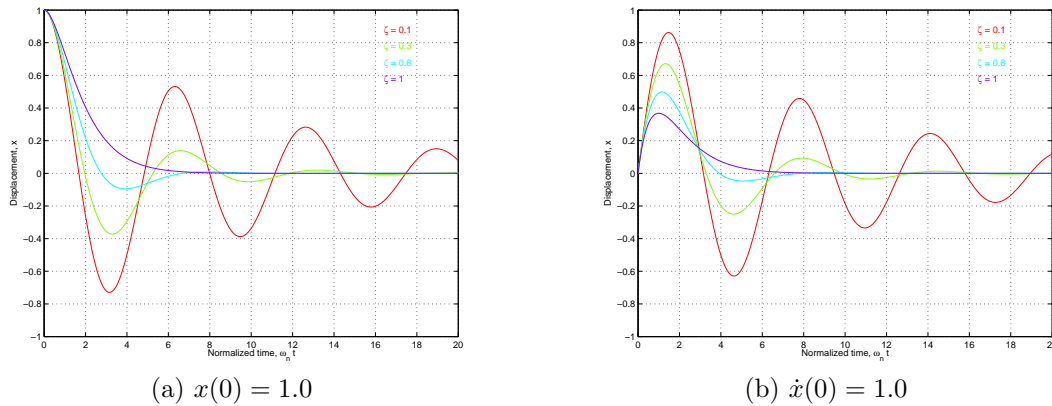


Figure 5.3: Underdamped response of spring-mass-damper system. (a) Displacement perturbation: $x(0) = 1.0$; $\dot{x}(0) = 0$. (b) Velocity perturbation: $\dot{x}(0) = 1.0$; $x(0) = 0$.

Since the determinant of the coefficient matrix in these equations is equal to $\omega_n \sqrt{1 - \zeta^2}$, the system is non-singular when $\zeta < 1$, and the solution is completely determined by the initial values of x and \dot{x} . Figure 5.3 shows the response of the underdamped system Eq. (5.16) for various values of the damping ratio, again as a function of the dimensionless time \hat{t} .

As is seen from Eq. (5.22), the solution consists of an exponentially decaying sinusoidal motion. This motion is characterized by its period and the rate at which the oscillations are damped. The period is given by

$$T = \frac{2\pi}{\omega_n \sqrt{1 - \zeta^2}} \quad (5.25)$$

and the time to damp to $1/n$ times the initial amplitude is given by¹

$$t_{1/n} = \frac{\ln n}{\omega_n \zeta} \quad (5.26)$$

For these oscillatory motions, the damping frequently is characterized by the *number of cycles* to damp to $1/n$ times the initial amplitude, which is given by

$$N_{1/n} = \frac{t_{1/n}}{T} = \frac{\ln n}{2\pi} \frac{\sqrt{1 - \zeta^2}}{\zeta} \quad (5.27)$$

Note that this latter quantity is independent of the undamped natural frequency; i.e., it depends *only* on the damping ratio ζ .

5.1.2 Systems of First-order Equations

Although the equation describing the spring-mass-damper system of the previous section was solved in its original form, as a single second-order ordinary differential equation, it is useful for later

¹The most commonly used values of n are 2 and 10, corresponding to the times to damp to $1/2$ the initial amplitude and $1/10$ the initial amplitude, respectively.

generalization to re-write it as a *system* of coupled first-order differential equations by defining

$$\begin{aligned} x_1 &= x \\ x_2 &= \frac{dx}{dt} \end{aligned} \quad (5.28)$$

Equation (5.8) can then be written as

$$\frac{d}{dt} \begin{pmatrix} x_1 \\ x_2 \end{pmatrix} = \begin{pmatrix} 0 & 1 \\ -\omega_n^2 & -2\zeta\omega_n \end{pmatrix} \begin{pmatrix} x_1 \\ x_2 \end{pmatrix} + \begin{pmatrix} 0 \\ \frac{1}{m} \end{pmatrix} F(t) \quad (5.29)$$

which has the general form

$$\dot{\mathbf{x}} = \mathbf{A}\mathbf{x} + \mathbf{B}\eta \quad (5.30)$$

where $\mathbf{x} = (x_1, x_2)^T$, the dot represents a time derivative, and $\eta(t) = F(t)$ will be identified as the control input.

The free response is then governed by the system of equations

$$\dot{\mathbf{x}} = \mathbf{A}\mathbf{x} \quad (5.31)$$

and substitution of the general form

$$\mathbf{x} = \mathbf{x}_i e^{\lambda_i t} \quad (5.32)$$

into Eqs. (5.31) requires

$$(\mathbf{A} - \lambda_i \mathbf{I}) \mathbf{x}_i = 0 \quad (5.33)$$

Thus, the free response of the system is seen to be completely determined by the eigenstructure (i.e., the eigenvalues and eigenvectors) of the *plant matrix* \mathbf{A} . The vector \mathbf{x}_i is seen to be the eigenvector associated with the eigenvalue λ_i of the matrix \mathbf{A} and, when the eigenvalues are unique, the general solution can be expressed as a linear combination of the form

$$\mathbf{x} = \sum_{i=1}^2 a_i \mathbf{x}_i e^{\lambda_i t} \quad (5.34)$$

where the constants a_i are determined by the initial conditions. The *modal matrix* \mathbf{Q} of \mathbf{A} is defined as the matrix whose columns are the eigenvectors of \mathbf{A}

$$\mathbf{Q} = (\mathbf{x}_1 \quad \mathbf{x}_2) \quad (5.35)$$

so the initial values of the vector \mathbf{x} are given by

$$\mathbf{x}(0) = \sum_{i=1}^2 a_i \mathbf{x}_i = \mathbf{Q}\mathbf{a} \quad (5.36)$$

where the elements of the vector

$$\mathbf{a} = \{a_1, a_2\}^T$$

correspond to the coefficients in the *modal expansion* of the solution in the form of Eq. (5.34). When the eigenvalues are complex, they must appear in complex conjugate pairs, and the corresponding eigenvectors also are complex conjugates, so the solution corresponding to a complex conjugate pair of eigenvalues again corresponds to an exponentially damped harmonic oscillation.

While the above analysis corresponds to the second-order system treated previously, the advantage of viewing it as a system of first-order equations is that, once we have shifted our viewpoint the analysis

carries through for a system of any order. In particular, the simplest complete linear analyses of either longitudinal or lateral/directional dynamics will lead to fourth-order systems – i.e., to systems of four coupled first-order differential equations. In practice, most of the required operations involving eigenvalues and eigenvectors can be accomplished easily using numerical software packages, such as MATLAB

5.2 Longitudinal Motions

In this section, we develop the small-disturbance equations for longitudinal motions in standard state-variable form. Recall that the linearized equations describing small longitudinal perturbations from a longitudinal equilibrium state can be written

$$\begin{aligned} & \left[\frac{d}{dt} - X_u \right] u + g_0 \cos \Theta_0 \theta - X_w w = X_{\delta_e} \delta_e + X_{\delta_T} \delta_T \\ -Z_u u + \left[(1 - Z_{\dot{w}}) \frac{d}{dt} - Z_w \right] w - [u_0 + Z_q] q + g_0 \sin \Theta_0 \theta &= Z_{\delta_e} \delta_e + Z_{\delta_T} \delta_T \\ -M_u u - \left[M_{\dot{w}} \frac{d}{dt} + M_w \right] w + \left[\frac{d}{dt} - M_q \right] q &= M_{\delta_e} \delta_e + M_{\delta_T} \delta_T \end{aligned} \quad (5.37)$$

If we introduce the longitudinal state variable vector

$$\mathbf{x} = [u \quad w \quad q \quad \theta]^T \quad (5.38)$$

and the longitudinal control vector

$$\boldsymbol{\eta} = [\delta_e \quad \delta_T]^T \quad (5.39)$$

these equations are equivalent to the system of first-order equations

$$\mathbf{I}_n \dot{\mathbf{x}} = \mathbf{A}_n \mathbf{x} + \mathbf{B}_n \boldsymbol{\eta} \quad (5.40)$$

where $\dot{\mathbf{x}}$ represents the time derivative of the state vector \mathbf{x} , and the matrices appearing in this equation are

$$\begin{aligned} \mathbf{A}_n &= \begin{pmatrix} X_u & X_w & 0 & -g_0 \cos \Theta_0 \\ Z_u & Z_w & u_0 + Z_q & -g_0 \sin \Theta_0 \\ M_u & M_w & M_q & 0 \\ 0 & 0 & 1 & 0 \end{pmatrix} \\ \mathbf{I}_n &= \begin{pmatrix} 1 & 0 & 0 & 0 \\ 0 & 1 - Z_{\dot{w}} & 0 & 0 \\ 0 & -M_{\dot{w}} & 1 & 0 \\ 0 & 0 & 0 & 1 \end{pmatrix}, \quad \mathbf{B}_n = \begin{pmatrix} X_{\delta_e} & X_{\delta_T} \\ Z_{\delta_e} & Z_{\delta_T} \\ M_{\delta_e} & M_{\delta_T} \\ 0 & 0 \end{pmatrix} \end{aligned} \quad (5.41)$$

It is not difficult to show that the inverse of \mathbf{I}_n is

$$\mathbf{I}_n^{-1} = \begin{pmatrix} 1 & 0 & 0 & 0 \\ 0 & \frac{1}{1 - Z_{\dot{w}}} & 0 & 0 \\ 0 & \frac{M_{\dot{w}}}{1 - Z_{\dot{w}}} & 1 & 0 \\ 0 & 0 & 0 & 1 \end{pmatrix} \quad (5.42)$$

so premultiplying Eq. (5.40) by \mathbf{I}_n^{-1} gives the standard form

$$\dot{\mathbf{x}} = \mathbf{A} \mathbf{x} + \mathbf{B} \boldsymbol{\eta} \quad (5.43)$$

where

$$\mathbf{A} = \begin{pmatrix} X_u & X_w & 0 & -g_0 \cos \Theta_0 \\ \frac{Z_u}{1-Z_{\dot{w}}} & \frac{Z_w}{1-Z_{\dot{w}}} & \frac{u_0+Z_q}{1-Z_{\dot{w}}} & \frac{-g_0 \sin \Theta_0}{1-Z_{\dot{w}}} \\ M_u + \frac{M_{\dot{w}}Z_u}{1-Z_{\dot{w}}} & M_w + \frac{M_{\dot{w}}Z_w}{1-Z_{\dot{w}}} & M_q + \frac{(u_0+Z_q)M_{\dot{w}}}{1-Z_{\dot{w}}} & \frac{-M_{\dot{w}}g_0 \sin \Theta_0}{1-Z_{\dot{w}}} \\ 0 & 0 & 1 & 0 \end{pmatrix} \quad (5.44)$$

$$\mathbf{B} = \begin{pmatrix} X_{\delta_e} & X_{\delta_T} \\ \frac{Z_{\delta_e}}{1-Z_{\dot{w}}} & \frac{Z_{\delta_T}}{1-Z_{\dot{w}}} \\ M_{\delta_e} + \frac{M_{\dot{w}}Z_{\delta_e}}{1-Z_{\dot{w}}} & M_{\delta_T} + \frac{M_{\dot{w}}Z_{\delta_T}}{1-Z_{\dot{w}}} \\ 0 & 0 \end{pmatrix}$$

Note that

$$Z_{\dot{w}} = \frac{QS\bar{c}}{2mu_0^2} \mathbf{C}_{Z\dot{\alpha}} = -\frac{1}{2\mu} \mathbf{C}_{L\dot{\alpha}} \quad (5.45)$$

and

$$Z_q = \frac{QS\bar{c}}{2mu_0} \mathbf{C}_{Zq} = -\frac{u_0}{2\mu} \mathbf{C}_{Lq} \quad (5.46)$$

Since the aircraft mass parameter μ is typically large (on the order of 100), it is common to neglect $Z_{\dot{w}}$ with respect to unity and to neglect Z_q relative to u_0 , in which case the matrices \mathbf{A} and \mathbf{B} can be approximated as

$$\mathbf{A} = \begin{pmatrix} X_u & X_w & 0 & -g_0 \cos \Theta_0 \\ Z_u & Z_w & u_0 & -g_0 \sin \Theta_0 \\ M_u + M_{\dot{w}}Z_u & M_w + M_{\dot{w}}Z_w & M_q + u_0M_{\dot{w}} & -M_{\dot{w}}g_0 \sin \Theta_0 \\ 0 & 0 & 1 & 0 \end{pmatrix} \quad (5.47)$$

$$\mathbf{B} = \begin{pmatrix} X_{\delta_e} & X_{\delta_T} \\ Z_{\delta_e} & Z_{\delta_T} \\ M_{\delta_e} + M_{\dot{w}}Z_{\delta_e} & M_{\delta_T} + M_{\dot{w}}Z_{\delta_T} \\ 0 & 0 \end{pmatrix}$$

This is the approximate form of the linearized equations for longitudinal motions as they appear in many texts (see, e.g., Eqs. (4.53) and (4.54) in [3]²).

The various dimensional stability derivatives appearing in Eqs. (5.44) and (5.47) are related to their dimensionless aerodynamic coefficient counterparts in Table 5.1; these data were also presented in Table 4.1 in the previous chapter.

5.2.1 Modes of Typical Aircraft

The natural response of most aircraft to longitudinal perturbations typically consists of two under-damped oscillatory modes having rather different time scales. One of the modes has a relatively short period and is usually quite heavily damped; this is called the *short period mode*. The other mode has a much longer period and is rather lightly damped; this is called the *phugoid mode*.

We illustrate this response using the stability derivatives for the Boeing 747 aircraft at its Mach 0.25 power approach configuration at standard sea-level conditions. The aircraft properties and flight

²The equations in [3] also assume level flight, or $\Theta_0 = 0$.

Variable	X	Z	M
u	$X_u = \frac{QS}{mu_0} [2\mathbf{C}_{X0} + \mathbf{C}_{Xu}]$	$Z_u = \frac{QS}{mu_0} [2\mathbf{C}_{Z0} + \mathbf{C}_{Zu}]$	$M_u = \frac{QS\bar{c}}{I_y u_0} \mathbf{C}_{mu}$
w	$X_w = \frac{QS}{mu_0} \mathbf{C}_{X\alpha}$	$Z_w = \frac{QS}{mu_0} \mathbf{C}_{Z\alpha}$	$M_w = \frac{QS\bar{c}}{I_y u_0} \mathbf{C}_{m\alpha}$
\dot{w}	$X_{\dot{w}} = 0$	$Z_{\dot{w}} = \frac{QS\bar{c}}{2mu_0^2} \mathbf{C}_{Z\dot{\alpha}}$	$M_{\dot{w}} = \frac{QS\bar{c}^2}{2I_y u_0^2} \mathbf{C}_{m\dot{\alpha}}$
q	$X_q = 0$	$Z_q = \frac{QS\bar{c}}{2mu_0} \mathbf{C}_{Zq}$	$M_q = \frac{QS\bar{c}^2}{2I_y u_0} \mathbf{C}_{mq}$

Table 5.1: Relation of dimensional stability derivatives for longitudinal motions to dimensionless derivatives of aerodynamic coefficients. The dimensionless coefficients on which these are based are described in Chapter 4.

condition are given by [2]

$$\begin{aligned}
 V &= 279.1 \text{ ft/sec}, & \rho &= 0.002377 \text{ slug/ft}^3 \\
 S &= 5,500. \text{ ft}^2, & \bar{c} &= 27.3 \text{ ft} \\
 W &= 564,032. \text{ lb}, & I_y &= 32.3 \times 10^6 \text{ slug-ft}^2
 \end{aligned} \tag{5.48}$$

and the relevant aerodynamic coefficients are

$$\begin{aligned}
 \mathbf{C}_L &= 1.108, & \mathbf{C}_D &= 0.102, & \Theta_0 &= 0 \\
 \mathbf{C}_{L\alpha} &= 5.70, & \mathbf{C}_{L\dot{\alpha}} &= 6.7, & \mathbf{C}_{Lq} &= 5.4, & \mathbf{C}_{LM} &= 0 \\
 \mathbf{C}_{D\alpha} &= 0.66, & & & & & &
 \end{aligned} \tag{5.49}$$

$$\begin{aligned}
 \mathbf{C}_{m\alpha} &= -1.26, & \mathbf{C}_{m\dot{\alpha}} &= -3.2, & \mathbf{C}_{mq} &= -20.8, & \mathbf{C}_{mM} &= 0
 \end{aligned} \tag{5.50}$$

These values correspond to the following dimensional stability derivatives

$$\begin{aligned}
 X_u &= -0.0212, & X_w &= 0.0466 \\
 Z_u &= -0.2306, & Z_w &= -0.6038, & Z_{\dot{w}} &= -0.0341, & Z_q &= -7.674 \\
 M_u &= 0.0, & M_w &= -0.0019, & M_{\dot{w}} &= -0.0002, & M_q &= -0.4381
 \end{aligned} \tag{5.51}$$

and the plant matrix is

$$\mathbf{A} = \begin{pmatrix} -0.0212 & 0.0466 & 0.000 & -32.174 \\ -0.2229 & -0.5839 & 262.472 & 0.0 \\ 0.0001 & -0.0018 & -0.5015 & 0.0 \\ 0.0 & 0.0 & 1.0 & 0.0 \end{pmatrix} \tag{5.52}$$

The characteristic equation is given by

$$|\mathbf{A} - \lambda\mathbf{I}| = \lambda^4 + 1.1066\lambda^3 + 0.7994\lambda^2 + 0.0225\lambda + 0.0139 = 0 \tag{5.53}$$

and its roots are

$$\begin{aligned}
 \lambda_{\text{sp}} &= -0.5515 \pm i 0.6880 \\
 \lambda_{\text{ph}} &= -0.00178 \pm i 0.1339
 \end{aligned} \tag{5.54}$$

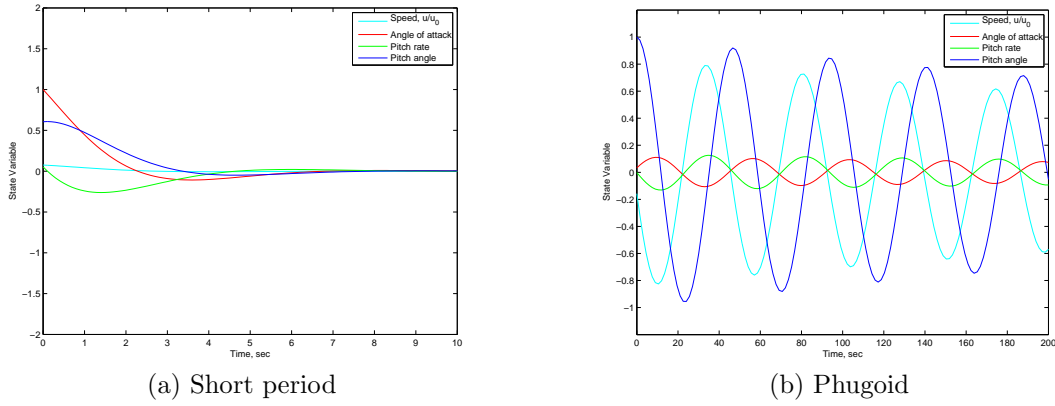


Figure 5.4: Response of Boeing 747 aircraft to longitudinal perturbations. (a) Short period response; (b) Phugoid response.

where, as suggested by the subscripts, the first pair of roots corresponds to the short period mode, and the second pair corresponds to the phugoid mode. The damping ratios of the two modes are thus given by

$$\zeta_{\text{sp}} = \sqrt{\frac{1}{1 + \left(\frac{\eta}{\xi}\right)_{\text{sp}}^2}} = \sqrt{\frac{1}{1 + \left(\frac{0.6880}{0.5515}\right)^2}} = 0.6255$$

$$\zeta_{\text{ph}} = \sqrt{\frac{1}{1 + \left(\frac{\eta}{\xi}\right)_{\text{ph}}^2}} = \sqrt{\frac{1}{1 + \left(\frac{0.1339}{0.00178}\right)^2}} = 0.0133$$
(5.55)

where ξ and η are the real and imaginary parts of the respective roots, and the undamped natural frequencies of the two modes are

$$\omega_{n_{\text{sp}}} = \frac{-\xi_{\text{sp}}}{\zeta_{\text{sp}}} = \frac{0.5515}{0.6255} = 0.882 \text{ sec}^{-1}$$

$$\omega_{n_{\text{ph}}} = \frac{-\xi_{\text{ph}}}{\zeta_{\text{ph}}} = \frac{0.00178}{0.0133} = 0.134 \text{ sec}^{-1}$$
(5.56)

The periods of the two modes are given by

$$T_{\text{sp}} = \frac{2\pi}{\omega_{n_{\text{sp}}} \sqrt{1 - \zeta_{\text{sp}}^2}} = 9.13 \text{ sec}$$
(5.57)

and

$$T_{\text{ph}} = \frac{2\pi}{\omega_{n_{\text{ph}}} \sqrt{1 - \zeta_{\text{ph}}^2}} = 46.9 \text{ sec}$$
(5.58)

respectively.

Figure 5.4 illustrates the short period and phugoid responses for the Boeing 747 under these conditions. These show the time histories of the state variables following an initial perturbation that is chosen to excite *only* the (a) short period mode or the (b) phugoid mode, respectively.

It should be noted that the dimensionless velocity perturbations u/u_0 and $\alpha = w/u_0$ are plotted in these figures, in order to allow comparisons with the other state variables. The plant matrix can be modified to reflect this choice of state variables as follows. The elements of the first two columns of the original plant matrix should be multiplied by u_0 , then the entire plant matrix should be premultiplied by the diagonal matrix having elements $\text{diag}(1/u_0, 1/u_0, 1, 1)$. The combination of these two steps is equivalent to dividing the elements in the upper right two-by-two block of the plant matrix \mathbf{A} by u_0 , and multiplying the elements in the lower left two-by-two block by u_0 . The resulting scaled plant matrix is then given by

$$\mathbf{A} = \begin{pmatrix} -0.0212 & 0.0466 & 0.000 & -0.1153 \\ -0.2229 & -0.5839 & 0.9404 & 0.0 \\ 0.0150 & -0.5031 & -0.5015 & 0.0 \\ 0.0 & 0.0 & 1.0 & 0.0 \end{pmatrix} \quad (5.59)$$

Note that, after this re-scaling, the magnitudes of the elements in the upper-right and lower-left two by two blocks of the plant matrix are more nearly the same order as the other terms (than they were in the original form).

It is seen in the figures that the short period mode is, indeed, rather heavily damped, while the phugoid mode is very lightly damped. In spite of the light damping of the phugoid, it generally does not cause problems for the pilot because its time scale is long enough that minor control inputs can compensate for the excitation of this mode by disturbances.

The relative magnitudes and phases of the perturbations in state variables for the two modes can be seen from the *phasor diagrams* for the various modes. These are plots in the complex plane of the components of the mode eigenvector corresponding to each of the state variables. The phasor plots for the short period and phugoid modes for this example are shown in Fig. 5.5. It is seen that the airspeed variation in the short period mode is, indeed, negligibly small, and the pitch angle θ lags the pitch rate q by substantially more than 90 degrees (due to the relatively large damping). The phugoid is seen to consist primarily of perturbations in airspeed and pitch angle. Although it is difficult to see on the scale of Fig. 5.5 (b), the pitch angle θ lags the pitch rate q by almost exactly 90 degrees for the phugoid (since the motion is so lightly damped it is nearly harmonic).

An arbitrary initial perturbation will generally excite both the short period and phugoid modes. This is illustrated in Fig. 5.6, which plots the time histories of the state variables following an initial perturbation in angle of attack. Figure 5.6 (a) shows the early stages of the response (on a time

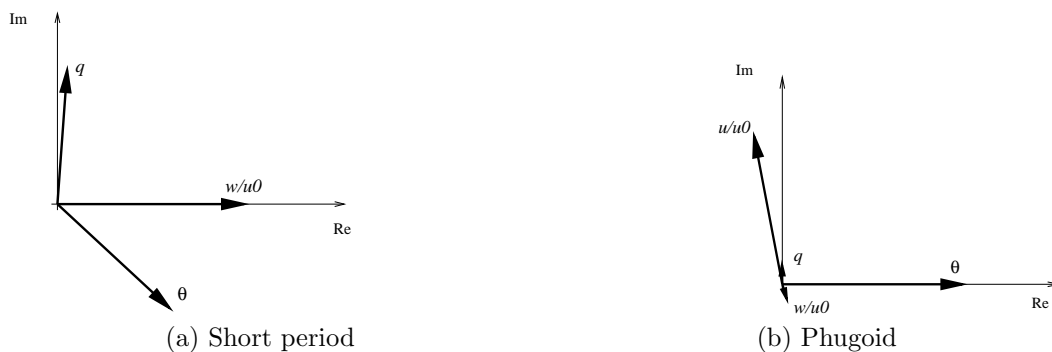


Figure 5.5: Phasor diagrams for longitudinal modes of the Boeing 747 aircraft in powered approach at $\mathbf{M} = 0.25$. Perturbation in normalized speed u/u_0 is too small to be seen in short period mode.

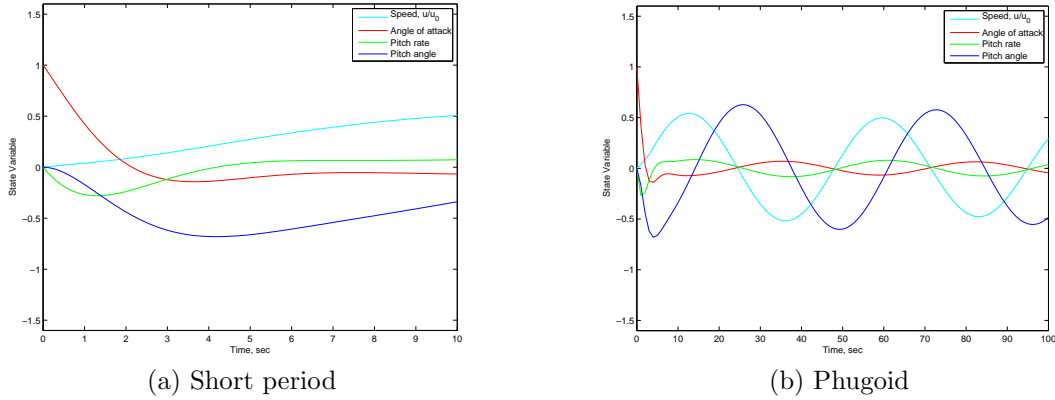


Figure 5.6: Response of Boeing 747 aircraft to unit perturbation in angle of attack. (a) Time scale chosen to emphasize short period response; (b) Time scale chosen to emphasize phugoid response.

scale appropriate for the short period mode), while Fig. 5.6 (b) shows the response on a time scale appropriate for describing the phugoid mode.

The pitch- and angle-of-attack-damping are important for damping the short period mode, while its frequency is determined primarily by the pitch stiffness. The period of the phugoid mode is nearly independent of vehicle parameters, and is very nearly inversely proportional to airspeed. The damping ratio for the phugoid is approximately proportional to the ratio C_D/C_L , which is small for efficient aircraft. These properties can be seen from the approximate analyses of the two modes presented in the following two sections.

5.2.2 Approximation to Short Period Mode

The short period mode typically occurs so quickly that it proceeds at essentially constant vehicle speed. A useful approximation for the mode can thus be developed by setting $u = 0$ and solving

$$\begin{aligned} (1 - Z_{\dot{w}}) \dot{w} &= Z_w w + (u_0 + Z_q) q \\ -M_{\dot{w}} \dot{w} + \dot{q} &= M_w w + M_q q \end{aligned} \quad (5.60)$$

which can be written in state-space form as

$$\frac{d}{dt} \begin{pmatrix} w \\ q \end{pmatrix} = \begin{pmatrix} \frac{Z_w}{1 - Z_{\dot{w}}} & \frac{u_0 + Z_q}{1 - Z_{\dot{w}}} \\ M_w + \frac{M_{\dot{w}} Z_w}{1 - Z_{\dot{w}}} & M_q + M_{\dot{w}} \frac{u_0 + Z_q}{1 - Z_{\dot{w}}} \end{pmatrix} \begin{pmatrix} w \\ q \end{pmatrix} \quad (5.61)$$

Since

$$\frac{Z_q}{u_0} = \frac{QS\bar{c}}{2mu_0^2} C_{Zq} = -\frac{\eta V_H a_t}{\mu} \quad (5.62)$$

where μ , the aircraft relative mass parameter, is usually large (on the order of one hundred), it is consistent with the level of our approximation to neglect Z_q relative to u_0 . Also, we note that

$$Z_{\dot{w}} = \frac{QS\bar{c}}{2mu_0^2} C_{Z\dot{\alpha}} = -\frac{\eta V_H a_t}{\mu} \frac{d\epsilon}{d\alpha} \quad (5.63)$$

is generally also very small. Thus, Eqs. (5.61) can be further approximated as

$$\frac{d}{dt} \begin{pmatrix} w \\ q \end{pmatrix} = \begin{pmatrix} Z_w & u_0 \\ M_w + M_{\dot{w}}Z_w & M_q + M_{\dot{w}}u_0 \end{pmatrix} \begin{pmatrix} w \\ q \end{pmatrix} \quad (5.64)$$

The characteristic equation for the simplified plant matrix of Eq. (5.64) is

$$\lambda^2 - (Z_w + M_q + u_0M_{\dot{w}})\lambda + Z_wM_q - u_0M_w = 0 \quad (5.65)$$

or, if the derivatives with respect to w are expressed as derivatives with respect to α ,

$$\lambda^2 - \left(M_q + M_{\dot{\alpha}} + \frac{Z_{\alpha}}{u_0} \right) \lambda - M_{\alpha} + \frac{Z_{\alpha}M_q}{u_0} = 0 \quad (5.66)$$

The undamped natural frequency and damping ratio for this motion are thus

$$\begin{aligned} \omega_n &= \sqrt{-M_{\alpha} + \frac{Z_{\alpha}M_q}{u_0}} \\ \zeta &= -\frac{M_q + M_{\dot{\alpha}} + \frac{Z_{\alpha}}{u_0}}{2\omega_n} \end{aligned} \quad (5.67)$$

Thus, it is seen that the undamped natural frequency of the mode is determined primarily by the pitch stiffness M_{α} , and the damping ratio is determined largely by the pitch- and angle-of-attack-damping.

For the example considered in the preceding sections of the Boeing 747 in powered approach we find

$$\begin{aligned} \omega_n &= \sqrt{0.54 + \frac{(-168.5)(-.4381)}{279.1}} \text{ sec}^{-1} = 0.897 \text{ sec}^{-1} \\ \zeta &= -\frac{-.4381 - .056 + \frac{(-168.5)}{279.1}}{2(0.897)} = 0.612 \end{aligned} \quad (5.68)$$

When these numbers are compared to $\omega_n = 0.882 \text{ sec}^{-1}$ and $\zeta = 0.6255$ from the more complete analysis (of the full fourth-order system), we see that the approximate analysis over predicts the undamped natural frequency by only about 1 per cent, and under predicts the damping ratio by less than 2 per cent. As will be seen in the next subsection when we consider approximating the phugoid mode, it generally is easier to approximate the large roots than the small ones, especially when the latter are lightly damped.

5.2.3 Approximation to Phugoid Mode

Since the phugoid mode typically proceeds at nearly constant angle of attack, and the motion is so slow that the pitch rate q is very small, we can approximate the behavior of the mode by writing only the X - and Z -force equations

$$\begin{aligned} \dot{u} &= X_u u + X_w w - g_0 \cos \Theta_0 \theta \\ (1 - Z_{\dot{w}}) \dot{w} &= Z_u u + Z_w w + (u_0 + Z_q) q - g_0 \sin \Theta_0 \theta \end{aligned} \quad (5.69)$$

which, upon setting $w = \dot{w} = 0$, can be written in the form

$$\frac{d}{dt} \begin{pmatrix} u \\ \theta \end{pmatrix} = \begin{pmatrix} X_u & -g_0 \cos \Theta_0 \\ -\frac{Z_u}{u_0 + Z_q} & \frac{g_0 \sin \Theta_0}{u_0 + Z_q} \end{pmatrix} \begin{pmatrix} u \\ \theta \end{pmatrix} \quad (5.70)$$

Since, as has been seen in Eq. (5.62), Z_q is typically very small relative to the speed u_0 , it is consistent with our neglect of \dot{q} and w also to neglect Z_q relative to u_0 . Also, we will consider only the case of level flight for the initial equilibrium, so $\Theta_0 = 0$, and Eq. (5.70) becomes

$$\frac{d}{dt} \begin{pmatrix} u \\ \theta \end{pmatrix} = \begin{pmatrix} X_u & -g_0 \\ -\frac{Z_u}{u_0} & 0 \end{pmatrix} \begin{pmatrix} u \\ \theta \end{pmatrix} \quad (5.71)$$

The characteristic equation for the simplified plant matrix of Eq. (5.71) is

$$\lambda^2 - X_u \lambda - \frac{g_0}{u_0} Z_u = 0 \quad (5.72)$$

The undamped natural frequency and damping ratio for this motion are thus

$$\begin{aligned} \omega_n &= \sqrt{-\frac{g_0}{u_0} Z_u} \\ \zeta &= \frac{-X_u}{2\omega_n} \end{aligned} \quad (5.73)$$

It is useful to express these results in terms of dimensionless aerodynamic coefficients. Recall that

$$Z_u = -\frac{QS}{mu_0} [2\mathbf{C}_{L0} + \mathbf{M}\mathbf{C}_{LM}] \quad (5.74)$$

and, for the case of a constant-thrust propulsive system,

$$X_u = -\frac{QS}{mu_0} [2\mathbf{C}_{D0} + \mathbf{M}\mathbf{C}_{DM}] \quad (5.75)$$

so, if we further neglect compressibility effects, we have

$$\begin{aligned} \omega_n &= \sqrt{2} \frac{g_0}{u_0} \\ \zeta &= \frac{1}{\sqrt{2}} \frac{\mathbf{C}_{D0}}{\mathbf{C}_{L0}} \end{aligned} \quad (5.76)$$

Thus, according to this approximation, the undamped natural frequency of the phugoid is a function only of the flight velocity, and the damping ratio is proportional to the drag-to-lift ratio. Since the latter quantity is small for an efficient flight vehicle, this explains why the phugoid typically is very lightly damped.

For the example of the Boeing 747 in powered approach we find

$$\begin{aligned} \omega_n &= \sqrt{2} \frac{32.174 \text{ ft/sec}^2}{279.1 \text{ ft/sec}} = 0.163 \text{ sec}^{-1} \\ \zeta &= \frac{1}{\sqrt{2}} \frac{0.102}{1.108} = 0.0651 \end{aligned} \quad (5.77)$$

When these numbers are compared to $\omega_n = 0.134 \text{ sec}^{-1}$ and $\zeta = 0.0133$ from the more complete analysis (of the full fourth-order system), we see that the approximate analysis over predicts the undamped natural frequency by about 20 per cent, and over predicts the damping ratio by a factor of almost 5. Nevertheless, this simplified analysis gives insight into the important parameters governing the mode.

5.2.4 Summary of Longitudinal Modes

We have seen that the response of a typical aircraft to longitudinal perturbations consists of two oscillatory modes:

1. A *short period* mode that usually is heavily damped, whose period is determined largely by the vehicle pitch stiffness $\mathbf{C}_{m\alpha}$, and which is damped primarily by pitch- and angle-of-attack-damping, \mathbf{C}_{mq} and $\mathbf{C}_{m\dot{\alpha}}$, respectively; and
2. A lightly damped, low frequency, *phugoid* mode whose period is nearly independent of vehicle parameters and inversely proportional to the flight velocity, and for which the damping ratio is proportional approximately to the ratio $\mathbf{C}_D/\mathbf{C}_L$, which is small for efficient vehicles.

We here illustrate the variation in response for a typical vehicle as a function of the vehicle static margin – which determines the pitch stiffness. The behavior of the roots of the characteristic equation of the complete fourth-order plant matrix is shown in Fig. 5.7 as a function of the pitch stiffness for our Boeing 747 example. The plot shows the locations of the roots as the static margin is reduced from an initial value of 0.22. As the c.g. is moved aft, both the phugoid and short period roots move toward the real axis. The short period mode becomes critically damped at a static margin of approximately 0.0158, and the phugoid becomes critically damped at a value of approximately 0.0021. One of the phugoid roots then moves toward the right-hand plane, and becomes neutrally stable at a static margin of 0.0. The other phugoid root moves to the left and, at a static margin of approximately -0.0145, joins one of the short-period roots to create another oscillatory mode, which is called the *third oscillatory mode*.

5.3 Lateral/Directional Motions

In this section, we develop the small-disturbance equations for lateral/directional motions in standard state-variable form. Recall that the linearized equations describing small lateral/directional perturbations from a longitudinal equilibrium state can be written

$$\begin{aligned} \left[\frac{d}{dt} - Y_v \right] v - Y_p p + [u_0 - Y_r] r - g_0 \cos \Theta_0 \phi &= Y_{\delta_r} \delta_r \\ -L_v v + \left[\frac{d}{dt} - L_p \right] p - \left[\frac{I_{xz}}{I_x} \frac{d}{dt} + L_r \right] r &= L_{\delta_r} \delta_r + L_{\delta_a} \delta_a \\ -N_v v - \left[\frac{I_{xz}}{I_z} \frac{d}{dt} + N_p \right] p + \left[\frac{d}{dt} - N_r \right] r &= N_{\delta_r} \delta_r + N_{\delta_a} \delta_a \end{aligned} \quad (5.78)$$

If we introduce the lateral/directional state variable vector

$$\mathbf{x} = [v \quad p \quad \phi \quad r]^T \quad (5.79)$$

and the lateral/directional control vector

$$\boldsymbol{\eta} = [\delta_r \quad \delta_a]^T \quad (5.80)$$

these equations are equivalent to the system of first-order equations

$$\mathbf{I}_n \dot{\mathbf{x}} = \mathbf{A}_n \mathbf{x} + \mathbf{B}_n \boldsymbol{\eta} \quad (5.81)$$

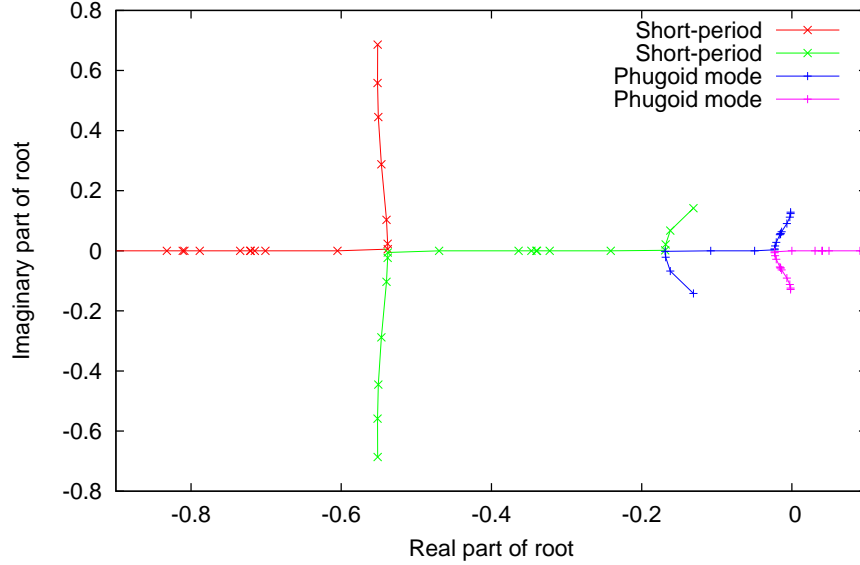


Figure 5.7: Locus of roots of longitudinal plant matrix for Boeing 747 in level flight at $\mathbf{M} = 0.25$ as standard sea level conditions as functions of c.g. location for values of static margin ranging from 0.22 to $-.05$. As the static margin is reduced, the roots of both oscillatory modes coalesce on the real axis; one of the phugoid roots moves to the right and becomes unstable, while the other moves to the left and joins with one of the short period roots to form a third oscillatory mode.

where $\dot{\mathbf{x}}$ represents the time derivative of the state vector \mathbf{x} , and the matrices appearing in this equation are

$$\mathbf{A}_n = \begin{pmatrix} Y_v & Y_p & g_0 \cos \Theta_0 & Y_r - u_0 \\ L_v & L_p & 0 & L_r \\ 0 & 1 & 0 & 0 \\ N_v & N_p & 0 & N_r \end{pmatrix} \quad (5.82)$$

$$\mathbf{I}_n = \begin{pmatrix} 1 & 0 & 0 & 0 \\ 0 & 1 & 0 & -i_x \\ 0 & 0 & 1 & 0 \\ 0 & -i_z & 0 & 1 \end{pmatrix}, \quad \mathbf{B}_n = \begin{pmatrix} Y_{\delta_r} & 0 \\ L_{\delta_r} & L_{\delta_a} \\ 0 & 0 \\ N_{\delta_r} & N_{\delta_a} \end{pmatrix}$$

where

$$i_x \equiv \frac{I_{xz}}{I_x}, \quad i_z \equiv \frac{I_{xz}}{I_z} \quad (5.83)$$

It is not difficult to show that the inverse of \mathbf{I}_n is

$$\mathbf{I}_n^{-1} = \begin{pmatrix} 1 & 0 & 0 & 0 \\ 0 & \frac{1}{1-i_x i_z} & 0 & \frac{i_x}{1-i_x i_z} \\ 0 & 0 & 1 & 0 \\ 0 & \frac{i_z}{1-i_x i_z} & 0 & \frac{1}{1-i_x i_z} \end{pmatrix} \quad (5.84)$$

so premultiplying Eq. (5.81) by \mathbf{I}_n^{-1} gives the standard form

$$\dot{\mathbf{x}} = \mathbf{A}\mathbf{x} + \mathbf{B}\eta$$

Variable	Y	L	N
v	$Y_v = \frac{QS}{mu_0} \mathbf{C}_{y\beta}$	$L_v = \frac{Q Sb}{I_x u_0} \mathbf{C}_{l\beta}$	$N_v = \frac{Q Sb}{I_z u_0} \mathbf{C}_{n\beta}$
p	$Y_p = \frac{Q Sb}{2mu_0} \mathbf{C}_{y_p}$	$L_p = \frac{Q Sb^2}{2I_x u_0} \mathbf{C}_{l_p}$	$N_p = \frac{Q Sb^2}{2I_z u_0} \mathbf{C}_{n_p}$
r	$Y_r = \frac{Q Sb}{2mu_0} \mathbf{C}_{y_r}$	$L_r = \frac{Q Sb^2}{2I_x u_0} \mathbf{C}_{l_r}$	$N_r = \frac{Q Sb^2}{2I_z u_0} \mathbf{C}_{n_r}$

Table 5.2: Relation of dimensional stability derivatives for lateral/directional motions to dimensionless derivatives of aerodynamic coefficients.

where

$$\begin{aligned}
 \mathbf{A} &= \begin{pmatrix} Y_v & Y_p & g_0 \cos \Theta_0 & Y_r - u_0 \\ \frac{L_v + i_x N_v}{1 - i_x i_z} & \frac{L_p + i_x N_p}{1 - i_x i_z} & 0 & \frac{L_r + i_x N_r}{1 - i_x i_z} \\ 0 & 1 & 0 & 0 \\ \frac{N_v + i_z L_v}{1 - i_x i_z} & \frac{N_p + i_z L_p}{1 - i_x i_z} & 0 & \frac{N_r + i_z L_r}{1 - i_x i_z} \end{pmatrix} \\
 \mathbf{B} &= \begin{pmatrix} Y_{\delta_r} & 0 \\ \frac{L_{\delta_r} + i_x N_{\delta_r}}{1 - i_x i_z} & \frac{L_{\delta_a} + i_x N_{\delta_a}}{1 - i_x i_z} \\ 0 & 0 \\ \frac{N_{\delta_r} + i_z L_{\delta_r}}{1 - i_x i_z} & \frac{N_{\delta_a} + i_z L_{\delta_a}}{1 - i_x i_z} \end{pmatrix}
 \end{aligned} \tag{5.85}$$

For most flight vehicles and situations, the ratios i_x and i_z are quite small. Neglecting these quantities with respect to unity allows us to write the \mathbf{A} and \mathbf{B} matrices for lateral directional motions as

$$\begin{aligned}
 \mathbf{A} &= \begin{pmatrix} Y_v & Y_p & g_0 \cos \Theta_0 & Y_r - u_0 \\ L_v & L_p & 0 & L_r \\ 0 & 1 & 0 & 0 \\ N_v & N_p & 0 & N_r \end{pmatrix} \\
 \mathbf{B} &= \begin{pmatrix} Y_{\delta_r} & 0 \\ L_{\delta_r} & L_{\delta_a} \\ 0 & 0 \\ N_{\delta_r} & N_{\delta_a} \end{pmatrix}
 \end{aligned} \tag{5.86}$$

This is the approximate form of the linearized equations for lateral/directional motions as they appear in many texts (see, e.g., Eqs. (5.33) in [3]).

The various dimensional stability derivatives appearing in Eqs. (5.85) and (5.86) are related to their dimensionless aerodynamic coefficient counterparts in Table 5.2; these data were also presented in Table 4.2 in the previous chapter.

5.3.1 Modes of Typical Aircraft

The natural response of most aircraft to lateral/directional perturbations typically consists of one damped oscillatory mode and two exponential modes, one of which is usually very heavily damped. The oscillatory mode has a relatively short period and can be relatively lightly damped, especially

for swept-wing aircraft; this is called the *Dutch Roll mode*, as the response consists of a combined rolling, sideslipping, yawing motion reminiscent of a (Dutch) speed-skater. One of the exponential modes is very heavily damped, and represents the response of the aircraft primarily in roll; it is called the *rolling mode*. The second exponential mode, called the *spiral mode*, can be either stable or unstable, but usually has a long enough time constant that it presents no difficulty for piloted vehicles, even when it is unstable.³

We illustrate this response again using the stability derivatives for the Boeing 747 aircraft at its Mach 0.25 powered approach configuration at standard sea-level conditions. This is the same vehicle and trim condition used to illustrate typical longitudinal behavior, and the basic aircraft properties and flight condition are given in Eq. (5.48). In addition, for the lateral/directional response we need the following vehicle parameters

$$\begin{aligned} W &= 564,032. \text{ lbf}, & b &= 195.7 \text{ ft} \\ I_x &= 14.3 \times 10^6 \text{ slug ft}^2, & I_z &= 45.3 \times 10^6 \text{ slug ft}^2, & I_{xz} &= -2.23 \times 10^6 \text{ slug ft}^2 \end{aligned} \quad (5.87)$$

and the aerodynamic derivatives

$$\begin{aligned} C_{y\beta} &= -.96 & C_{y_p} &= 0.0 & C_{y_r} &= 0.0 \\ C_{l\beta} &= -.221 & C_{l_p} &= -.45 & C_{l_r} &= 0.101 \\ C_{n\beta} &= 0.15 & C_{n_p} &= -.121 & C_{n_r} &= -.30 \end{aligned} \quad (5.88)$$

These values correspond to the following dimensional stability derivatives

$$\begin{aligned} Y_v &= -0.0999, & Y_p &= 0.0, & Y_r &= 0.0 \\ L_v &= -0.0055, & L_p &= -1.0994, & L_r &= 0.2468 \\ N_v &= 0.0012, & N_p &= -.0933, & N_r &= -.2314 \end{aligned} \quad (5.89)$$

and the dimensionless product of inertia factors are

$$i_x = -.1559, \quad i_z = -.0492 \quad (5.90)$$

Using these values, the plant matrix is found to be

$$\mathbf{A} = \begin{pmatrix} -0.0999 & 0.0000 & 32.174 & -279.10 \\ -0.0057 & -1.0932 & 0.0 & 0.2850 \\ 0.0 & 1.0 & 0.0 & 0.0 \\ 0.0015 & -.0395 & 0.0 & -.2454 \end{pmatrix} \quad (5.91)$$

The characteristic equation is given by

$$|\mathbf{A} - \lambda\mathbf{I}| = \lambda^4 + 1.4385\lambda^3 + 0.8222\lambda^2 + 0.7232\lambda + 0.0319 = 0 \quad (5.92)$$

and its roots are

$$\begin{aligned} \lambda_{\text{DR}} &= -.08066 \pm i 0.7433 \\ \lambda_{\text{roll}} &= -1.2308 \\ \lambda_{\text{spiral}} &= -.04641 \end{aligned} \quad (5.93)$$

³This is true at least when flying under visual flight rules and a horizontal reference is clearly visible. Under instrument flight rules pilots must learn to trust the artificial horizon indicator to avoid entering an unstable spiral.

where, as suggested by the subscripts, the first pair of roots corresponds to the Dutch Roll mode, and the real roots corresponds to the rolling and spiral modes, respectively.

The damping ratio of the Dutch Roll mode is thus given by

$$\zeta_{\text{DR}} = \sqrt{\frac{1}{1 + \left(\frac{\eta}{\xi}\right)_{\text{DR}}^2}} = \sqrt{\frac{1}{1 + \left(\frac{0.7433}{0.08066}\right)^2}} = 0.1079 \quad (5.94)$$

and the undamped natural frequency of the mode is

$$\omega_{n_{\text{DR}}} = \frac{-\xi_{\text{DR}}}{\zeta_{\text{DR}}} = \frac{0.08066}{0.1079} = 0.7477 \text{ sec}^{-1} \quad (5.95)$$

The period of the Dutch Roll mode is then given by

$$T_{\text{DR}} = \frac{2\pi}{\omega_n \sqrt{1 - \zeta^2}} = \frac{2\pi}{0.7477 \sqrt{1 - 0.1079^2}} = 8.45 \text{ sec} \quad (5.96)$$

and the number of cycles to damp to half amplitude is

$$N_{1/2_{\text{DR}}} = \frac{\ln 2}{2\pi} \frac{\sqrt{1 - \zeta^2}}{\zeta} = \frac{\ln 2}{2\pi} \frac{\sqrt{1 - 0.1079^2}}{0.1079} = 1.016 \quad (5.97)$$

Thus, the period of the Dutch Roll mode is seen to be on the same order as that of the longitudinal short period mode, but is much more lightly damped.

The times to damp to half amplitude for the rolling and spiral modes are seen to be

$$t_{1/2_{\text{roll}}} = \frac{\ln 2}{-\xi_{\text{roll}}} = \frac{\ln 2}{1.2308} = 0.563 \text{ sec} \quad (5.98)$$

and

$$t_{1/2_{\text{spiral}}} = \frac{\ln 2}{-\xi_{\text{spiral}}} = \frac{\ln 2}{0.04641} = 14.93 \text{ sec} \quad (5.99)$$

respectively.

The responses characteristic of these three modes are illustrated in Fig. 5.8. The figure shows the time histories of the state variables following initial perturbations that are designed to excite only a single mode. For each of the three subfigures the initial perturbation has unit amplitude for the largest component and is parallel to the corresponding eigenvector in the state space.

Here the first state variable is again plotted in dimensionless form as $\beta = v/u_0$. The plant matrix can be modified to reflect this change in state variable as follows. The first column of the original plant matrix is first multiplied by u_0 , then the entire plant matrix is pre-multiplied by the diagonal matrix having elements $\text{diag}(1/u_0, 1, 1, 1)$. This is equivalent to dividing all but the first element in the first row by u_0 , and multiplying all but the first element in the first column by u_0 . The first element in the first column remains unchanged. With this re-scaling the plant matrix becomes

$$\mathbf{A} = \begin{pmatrix} -0.0999 & 0.0000 & 0.1153 & -1.0000 \\ -1.6038 & -1.0932 & 0.0 & 0.2850 \\ 0.0 & 1.0 & 0.0 & 0.0 \\ 0.4089 & -0.0395 & 0.0 & -0.2454 \end{pmatrix} \quad (5.100)$$

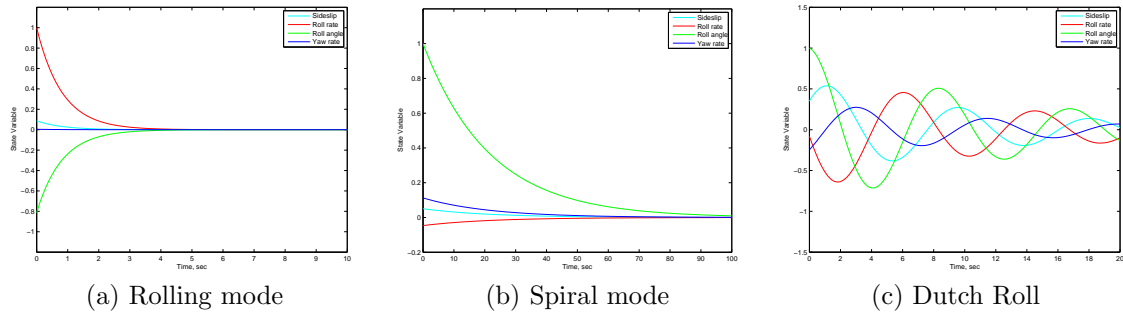


Figure 5.8: Response of Boeing 747 aircraft to unit perturbation in eigenvectors corresponding to the three lateral/directional modes of the vehicle. (a) Rolling mode; (b) Spiral mode; and (c) Dutch Roll mode.

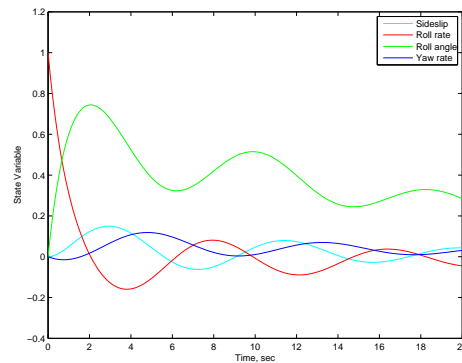


Figure 5.9: Response of Boeing 747 aircraft to unit perturbation in roll rate. Powered approach at $M = 0.25$ under standard sea-level conditions.

Note that, after this re-scaling, the magnitudes of the elements in the first row and first column of the plant matrix are more nearly the same order as the other terms (than they were in the original form).

It is seen that the rolling mode consists of almost pure rolling motion (with a very small amount of sideslip). The spiral mode consists of mostly coordinated roll and yaw. And for the the Dutch Roll mode, all the state variables participate, so the motion is characterized by coordinated rolling, sideslipping, and yawing motions.

An arbitrary initial perturbation will generally excite all three modes. This is illustrated in Fig. 5.9 which plots the time histories of the state variables following an initial perturbation in roll rate. The roll rate is seen to be quickly damped, leaving a slowly decaying spiral mode (appearing primarily in the roll angle), with the oscillatory Dutch Roll mode superimposed.

The phasor plots for the rolling and spiral modes are relatively uninteresting, since these correspond to real roots. The eigenvector amplitudes, however, show that the rolling mode is dominated by perturbations in bank angle ϕ and roll rate p , with a very small amount of sideslip and negligible yaw rate. The spiral mode is dominated by changes in bank angle. Since the motion is so slow, the roll rate is quite small, and the yaw rate is almost 2.5 times the roll rate, so we would expect significant changes in heading, as well as bank angle. The phasor diagram for the Dutch Roll mode

is shown in Fig. 5.10. Note that all four state variables participate with significant amplitudes in the Dutch Roll, and that the bank angle ϕ lags the roll rate p by almost exactly 90 degrees, as the motion is very lightly damped. Active control, usually to supply additional yaw damping, is often required on swept-wing transports to bring the damping of this mode to within acceptable limits.

5.3.2 Approximation to Rolling Mode

It has been seen that the rolling mode typically corresponds to almost pure roll. Thus, it is reasonable to neglect all equations except the rolling moment equation, and all perturbations except p . We thus approximate the rolling mode by the single first-order equation

$$\dot{p} = \frac{L_p + i_x N_p}{1 - i_x i_z} p \quad (5.101)$$

for which the characteristic value is

$$\lambda = \frac{L_p + i_x N_p}{1 - i_x i_z} \quad (5.102)$$

Since the product of inertia coefficients i_x and i_z usually are small, the rolling mode is seen to be dominated by roll damping L_p , which is almost always large and negative.

For our example of the Boeing 747 in powered approach at $\mathbf{M} = 0.25$, using the values from Eqs. (5.89) and (5.90), the approximate formula gives

$$\lambda = \frac{-1.0994 + (-.1559)(-.0933)}{1 - (-.1559)(-.0492)} \text{ sec}^{-1} = -1.093 \text{ sec}^{-1} \quad (5.103)$$

which is a bit more than 10 per cent less than the value of -1.2308 from the analysis for the full fourth-order system.

5.3.3 Approximation to Spiral Mode

The spiral mode consists of a slow rolling/yawing motion for which the sideslip is relatively small. The roll rate is quite small compared to the yaw rate, so a reasonable approximation is to set

$$\frac{dp}{dt} = 0 = \frac{L_v + i_x N_v}{1 - i_x i_z} v + \frac{L_r + i_x N_r}{1 - i_x i_z} r \quad (5.104)$$

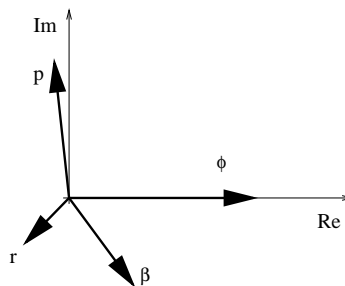


Figure 5.10: Phasor diagram for Dutch Roll mode of the Boeing 747 aircraft in powered approach at $\mathbf{M} = 0.25$.

whence

$$v \approx -\frac{L_r + i_x N_r}{L_v + i_x N_v} r \quad (5.105)$$

Since i_x and i_z are generally very small, this can be approximated as

$$v \approx -\frac{L_r}{L_v} r \quad (5.106)$$

The yaw equation

$$\frac{dr}{dt} = \frac{N_v + i_z L_v}{1 - i_x i_z} v + \frac{N_r + i_z L_r}{1 - i_x i_z} r \quad (5.107)$$

upon substitution of Eq. (5.106) and neglect of the product of inertia terms can then be written

$$\frac{dr}{dt} = \left(N_r - \frac{L_r N_v}{L_v} \right) r \quad (5.108)$$

so the root of the characteristic equation for the spiral mode is

$$\lambda = N_r - \frac{L_r N_v}{L_v} \quad (5.109)$$

Thus, it is seen that, according to this approximation, the spiral mode is stabilized by yaw damping N_r . Also, since stable dihedral effect corresponds to negative L_v and weathercock stability N_v and roll due to yaw rate L_r are always positive, the second term in Eq. (5.109) is destabilizing; thus increasing weathercock destabilizes the spiral mode while increasing dihedral effect stabilizes it.⁴

For our example of the Boeing 747 in powered approach at $\mathbf{M} = 0.25$, using the values from Eqs. (5.89) and (5.90), the approximate formula gives

$$\lambda = -.2314 - \frac{0.2468}{-.0055}(0.0012) = -.178 \quad (5.110)$$

which is almost four times the value of -.0464 from the analysis of the full fourth-order system. This is consistent with the usual difficulty in approximating small roots, but Eq. (5.109) still gives useful qualitative information about the effects of weathercock and dihedral stability on the spiral mode.

5.3.4 Approximation to Dutch Roll Mode

The Dutch Roll mode is particularly difficult to approximate because it usually involves significant perturbations in all four state variables. The most useful approximations require neglecting either the roll component or simplifying the sideslip component by assuming the vehicle c.g. travels in a straight line. This latter approximation means that $\psi = -\beta$, or

$$r = -\frac{\dot{v}}{u_0} \quad (5.111)$$

The roll and yaw moment equations (neglecting the product of inertia terms i_x and i_z) can then be written as

$$\frac{d}{dt} \begin{pmatrix} p \\ r \end{pmatrix} = \begin{pmatrix} L_v & L_p & L_r \\ N_v & N_p & N_r \end{pmatrix} \begin{pmatrix} v \\ p \\ r \end{pmatrix} \quad (5.112)$$

⁴Even if the spiral mode is unstable, its time constant usually is long enough that the pilot has no trouble countering it. Unpiloted aircraft, however, must have a stable spiral mode, which accounts for the excessive dihedral usually found on free-flight model aircraft.

Introduction of Eq. (5.111) completes this equation system in the form

$$\frac{d}{dt} \begin{pmatrix} v \\ p \\ r \end{pmatrix} = \begin{pmatrix} 0 & 0 & -u_0 \\ L_v & L_p & L_r \\ N_v & N_p & N_r \end{pmatrix} \begin{pmatrix} v \\ p \\ r \end{pmatrix} \quad (5.113)$$

The characteristic equation for this system is

$$\lambda^3 - (L_p + N_r)\lambda^2 + (L_p N_r + u_0 N_v - L_r N_p)\lambda + u_0(L_v N_p - L_p N_v) = 0 \quad (5.114)$$

This is still a cubic equation, however, for which there is no general closed-form solution. A useful approach to cubic equations that have a lightly damped oscillatory mode is Bairstow's approximation, which proceeds as follows. If the general cubic

$$\lambda^3 + a_2\lambda^2 + a_1\lambda + a_0 = 0 \quad (5.115)$$

has a lightly damped oscillatory mode, its undamped natural frequency can be approximated as

$$a_2\lambda^2 + a_0 \approx 0 \quad \text{or} \quad \lambda^2 \approx -\frac{a_0}{a_2} \quad (5.116)$$

This can then be used to write the first term of Eq. (5.115) as

$$-\frac{a_0}{a_2}\lambda + a_2\lambda^2 + a_1\lambda + a_0 = 0 \quad (5.117)$$

giving

$$a_2\lambda^2 + \left(a_1 - \frac{a_0}{a_2}\right)\lambda + a_0 = 0 \quad (5.118)$$

This quadratic equation can be solved in closed form (or at least the terms contributing to the undamped natural frequency and the damping ratio can be identified directly).

Applying Bairstow's approximation to Eq. (5.114) yields

$$\lambda^2 - \left[\frac{L_p N_r + u_0 N_v - L_r N_p}{L_p + N_r} + \frac{u_0(L_v N_p - L_p N_v)}{(L_p + N_r)^2} \right] \lambda + \frac{u_0(L_p N_v - L_v N_p)}{L_p + N_r} = 0 \quad (5.119)$$

Thus, the undamped natural frequency is given by

$$\omega_n^2 = \frac{u_0(L_p N_v - L_v N_p)}{L_p + N_r} \quad (5.120)$$

Since N_p is usually negative, both terms in the numerator have the same sign for stable dihedral. Thus, increasing either weathercock stability N_v or dihedral effect L_v increases the natural frequency of the motion.

The damping ratio is seen to be proportional to

$$2\zeta\omega_n = \frac{-L_p N_r - u_0 N_v + L_r N_p}{L_p + N_r} + \frac{u_0(-L_v N_p + L_p N_v)}{(L_p + N_r)^2} \quad (5.121)$$

For most aircraft, the ratio N_r/L_p is small, and expanding Eq. (5.121) in powers of this parameter and keeping only leading order terms gives

$$2\zeta\omega_n \approx -N_r \left(1 + \frac{u_0}{L_p^2} N_v\right) + \frac{N_p}{L_p} \left(L_r - \frac{u_0}{L_p} L_v\right) \quad (5.122)$$

Yaw damping is thus seen to contribute to positive ζ and be stabilizing, and weathercock stability N_v augments this effect. Since both N_p and L_p usually are negative, however, the dihedral effect L_v is seen to destabilize the Dutch Roll mode.⁵

For our example of the Boeing 747 in powered approach at $\mathbf{M} = 0.25$, using the values from Eqs. (5.89) and (5.90), the approximate formulas give

$$\omega_n = \left[\frac{(279.1) [(-1.0994)(0.0012) - (-.0055)(-.0933)]}{-1.0994 - .2314} \text{sec}^{-2} \right]^{1/2} = 0.620 \text{sec}^{-1} \quad (5.123)$$

and

$$\begin{aligned} \zeta &= - \frac{\frac{(-1.0994)(-.2314) - (.2468)(-.0933) + (279.1)(0.0012)}{-1.0994 - .2314} + (279.1) \frac{(-.0055)(-.0933) - (-1.0994)(0.0012)}{(-1.0994 - .2314)^2}}{2(0.620)} \\ &= 0.138 \end{aligned} \quad (5.124)$$

The approximation for the undamped natural frequency is only about 15 per cent less than the exact value of 0.748, but the exact damping ratio of 0.1079 is over predicted by almost 30 per cent. Nevertheless, the approximate Eq. (5.122) gives useful qualitative information about the effect of dihedral and weathercock on the damping of the mode.

5.3.5 Summary of Lateral/Directional Modes

We have seen that the response of a typical aircraft to lateral/directional perturbations consists of two exponential modes and one oscillatory mode:

1. A *rolling* mode that usually is heavily damped, whose time to damp to half amplitude is determined largely by the roll damping L_p ;
2. A *spiral* mode that usually is only lightly damped, or may even be unstable. Dihedral effect is an important stabilizing influence, while weathercock stability is destabilizing, for this mode; and
3. A lightly damped oscillatory, intermediate frequency *Dutch Roll* mode, which consists of a coordinated yawing, rolling, sideslipping motion. For this mode, dihedral effect is generally destabilizing, while weathercock stability is stabilizing.

Thus, the effects of weathercock and dihedral stability are reversed for the spiral and Dutch Roll modes, and compromise is required. We here present root locus plots illustrating this behavior for the full fourth-order system, corresponding to our example Boeing 747 vehicle in powered approach at standard sea level conditions at $\mathbf{M} = 0.25$. Figure 5.11 shows the locus of the roots of the plant matrix as the dihedral effect $\mathbf{C}_{l\beta}$ is increased from -.041 to -.561. As the dihedral effect is increased (i.e., made more negative) the spiral and rolling mode roots move to the left, while the complex

⁵Recall that there are two contributions from the wing to the yaw-due-to-roll derivative N_p ; profile drag contributes to positive N_p , while induced drag contributes to negative N_p . At low values of lift coefficient (i.e., high speeds) the profile drag contribution can dominate, in which case N_p becomes positive. In this case, increased dihedral effect can improve damping of the Dutch Roll mode. Consistent with this observation is the fact that Dutch Roll tends to be a more serious problem at low speeds.

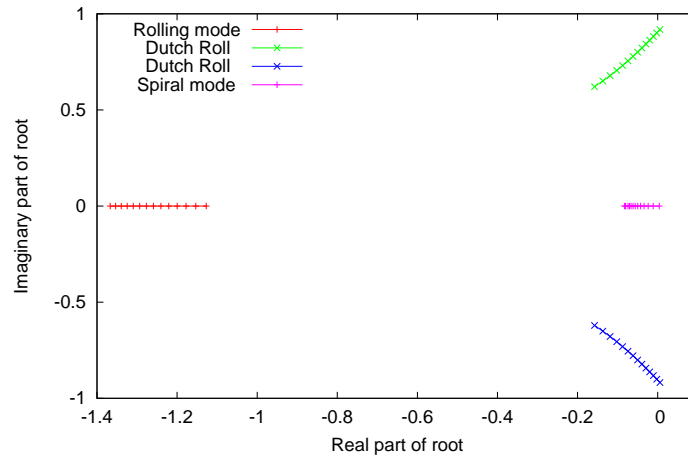


Figure 5.11: Locus of roots of plant matrix for Boeing 747 aircraft in powered approach at $M = 0.25$ under standard sea-level conditions. Dihedral effect is varied from -0.041 to -0.561 in steps of -0.04 , while all other stability derivatives are held fixed at their nominal values. Rolling and spiral modes become increasingly stable as dihedral effect is increased; spiral mode becomes stable at approximately $C_{l\beta} = -0.051$. Dutch Roll mode becomes less stable as dihedral effect is increased and becomes unstable at approximately $C_{l\beta} = -0.532$.

pair corresponding to the Dutch Roll mode moves to the right. Consistent with our approximate analysis, increasing the dihedral effect is seen to increase the natural frequency of the Dutch Roll mode.

Figure 5.12 shows the locus of the roots of the plant matrix as the weathercock stability coefficient $C_{n\beta}$ is increased from -0.07 to 0.69 . As the weathercock stability is increased (i.e., made more positive) the spiral and rolling mode roots move to the right, while the complex conjugate pair of roots corresponding to the Dutch Roll mode moves to the left. Again, consistent with our approximate analysis, increasing the weathercock stability increases the natural frequency of the Dutch Roll mode.

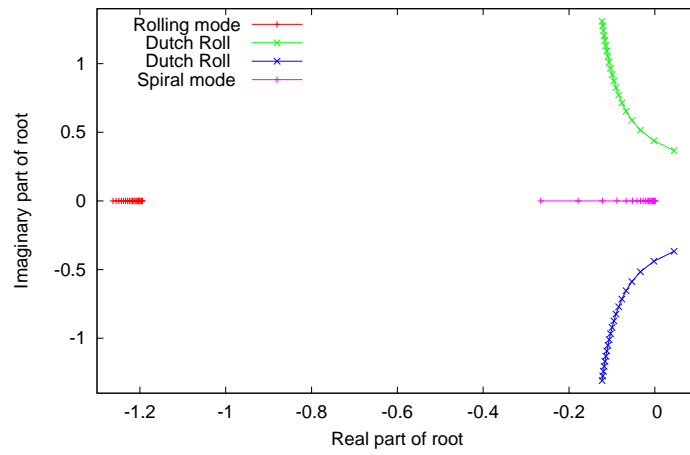


Figure 5.12: Locus of roots of plant matrix for Boeing 747 aircraft in powered approach at $\mathbf{M} = 0.25$ under standard sea-level conditions. Weathercock stability is varied from -0.07 to 0.69 in steps of 0.04 , while all other stability derivatives are held fixed at their nominal values. Rolling and spiral modes become less stable as weathercock stability is increased; spiral mode becomes unstable at approximately $\mathbf{C}_{n\beta} = 0.6567$. Dutch roll mode becomes increasingly stable as weathercock stability is increased, but is unstable for less than about $\mathbf{C}_{n\beta} = -0.032$.

5.4 Stability Characteristics of the Boeing 747

5.4.1 Longitudinal Stability Characteristics

In this section we summarize the longitudinal mass distribution and aerodynamic stability characteristics of a large, jet transport aircraft, the Boeing 747, at selected flight conditions. Data are summarized from the report by Heffley et al. [2]. Values for aerodynamic coefficients were scaled directly from plots of these variables, except for the derivatives C_{L_q} and $C_{L_{\dot{\alpha}}}$ for which no data are provided. These values were computed from the values of the corresponding dimensional stability derivatives Z_q and $Z_{\dot{w}}$, which are provided in tabular form, with the sign of $Z_{\dot{w}}$ changed to correct a seemingly obvious error.

Condition numbers correspond to those in the report; Conditions 5-10 are for a clean aircraft, Condition 2 corresponds to a powered approach with gear up and 20° flaps. Angles of attack are with respect to the fuselage reference line.

Condition	2	5	7	9	10
h (ft)	SL	20,000	20,000	40,000	40,000
M_∞	0.25	0.500	0.800	0.800	0.900
α (degrees)	5.70	6.80	0.0	4.60	2.40
W (lbf)	564,032.	636,636.	636,636.	636,636.	636,636.
I_y (slug-ft ²)	32.3×10^6	33.1×10^6	33.1×10^6	33.1×10^6	33.1×10^6
C_L	1.11	0.680	0.266	0.660	0.521
C_D	0.102	0.0393	0.0174	0.0415	0.0415
C_{L_α}	5.70	4.67	4.24	4.92	5.57
C_{D_α}	0.66	0.366	0.084	0.425	0.527
C_{m_α}	-1.26	-1.146	-0.629	-1.033	-1.613
$C_{L_{\dot{\alpha}}}$	6.7	6.53	5.99	5.91	5.53
$C_{m_{\dot{\alpha}}}$	-3.2	-3.35	-5.40	-6.41	-8.82
C_{L_q}	5.40	5.13	5.01	6.00	6.94
C_{m_q}	-20.8	-20.7	-20.5	-24.0	-25.1
C_{L_M}	0.0	-0.0875	0.105	0.205	-0.278
C_{D_M}	0.0	0.0	0.008	0.0275	0.242
C_{m_M}	0.0	0.121	-0.116	0.166	-0.114
$C_{L_{\delta_e}}$	0.338	0.356	0.270	0.367	0.300
$C_{m_{\delta_e}}$	-1.34	-1.43	-1.06	-1.45	-1.20

Table 5.3: Longitudinal mass properties and aerodynamic stability derivatives for the Boeing 747 at selected flight conditions.

5.4.2 Lateral/Directional Stability Characteristics

In this section we summarize the lateral/directional mass distribution and aerodynamic stability characteristics of a large, jet transport aircraft, the Boeing 747, at selected flight conditions. Data are summarized from the report by Heffley et al. [2]. Values for aerodynamic coefficients were scaled directly from plots of these variables.

Condition numbers correspond to those in the report; Conditions 5-10 are for a clean aircraft, Condition 2 corresponds to a powered approach with gear up and 20° flaps. Moments and products of inertia are with respect to stability axes for the given flight condition. Angles of attack are with respect to the fuselage reference line.

Condition	2	5	7	9	10
h (ft)	SL	20,000	20,000	40,000	40,000
M_∞	0.25	0.500	0.800	0.800	0.900
α (degrees)	5.70	6.80	0.0	4.60	2.40
W (lbf)	564,032.	636,636.	636,636.	636,636.	636,636.
I_x (slug-ft ²)	14.3×10^6	18.4×10^6	18.2×10^6	18.2×10^6	18.2×10^6
I_z (slug-ft ²)	45.3×10^6	49.5×10^6	49.7×10^6	49.7×10^6	49.7×10^6
I_{xz} (slug-ft ²)	-2.23×10^6	-2.76×10^6	0.97×10^6	-1.56×10^6	-0.35×10^6
$C_{y\beta}$	-.96	-.90	-.81	-.88	-.92
$C_{l\beta}$	-.221	-.193	-.164	-.277	-.095
$C_{n\beta}$	0.150	0.147	0.179	0.195	0.207
C_{l_p}	-.45	-.323	-.315	-.334	-.296
C_{n_p}	-.121	-.0687	0.0028	-.0415	0.0230
C_{l_r}	0.101	0.212	0.0979	0.300	0.193
C_{n_r}	-.30	-.278	-.265	-.327	-.333
$C_{l_{\delta_a}}$	0.0461	0.0129	0.0120	0.0137	0.0139
$C_{n_{\delta_a}}$	0.0064	0.0015	0.0008	0.0002	-.0027
$C_{y_{\delta_r}}$	0.175	0.1448	0.0841	0.1157	0.0620
$C_{l_{\delta_r}}$	0.007	0.0039	0.0090	0.0070	0.0052
$C_{n_{\delta_r}}$	-.109	-.1081	-.0988	-.1256	-.0914

Table 5.4: Lateral/Directional mass properties and aerodynamic stability derivatives for the Boeing 747 at selected flight conditions.

Bibliography

- [1] Bernard Etkin & Lloyd Duff Reid, **Dynamics of Flight, Stability and Control**, McGraw-Hill, Third Edition, 1996.
- [2] R. K. Heffley & W. F. Jewell, **Aircraft Handling Qualities Data**, NASA CR-2144, December 1972.
- [3] Robert C. Nelson, **Aircraft Stability and Automatic Control**, McGraw-Hill, Second edition, 1998.
- [4] Louis V. Schmidt, **Introduction to Aircraft Flight Dynamics**, AIAA Education Series, 1998.